International Geology Review, Vol. 47, 2005, p. 952–970.

Rare-Earth Element, Lead, Carbon, and Nitrogen Geochemistry of Apatite-Bearing Metasediments from the ~3.8 Ga Isua Supracrustal Belt, West Greenland

MANABU NISHIZAWA,[1] NAOTO TAKAHATA,

Center for Advanced Marine Research, Ocean Research Institute, University of Tokyo, Minamidai 1-15-1, Nakanoku, Tokyo 164-8639, Japan

KENTARO TERADA,

Department of Earth and Planetary Sciences, Hiroshima University, Kagami-yama 1-3-1, Higashi-Hiroshima, 739-8526, Japan

TSUYOSHI KOMIYA,

Department of Earth and Planetary Sciences, Tokyo Institute of Technology, Ookayama 2-12-1, Meguroku, Tokyo, 152-8551, Japan

YUICHIRO UENO,

Research Center for the Evolving Earth and Planets, Department of Environmental Science and Technology, Tokyo Institute of Technology, Post No. S2-17, Midori-ku, Yokohama 226-8503, Japan

AND YUJI SANO

Center for Advanced Marine Research, Ocean Research Institute, University of Tokyo, Minamidai 1-15-1, Nakanoku, Tokyo 164-8639, Japan

Abstract

We performed rare-earth element (REE) geochemistry and U-Pb geochronology on apatites in metasediments from the ~3.8 Ga Isua supracrustal belt (ISB) and Akilia Island, West Greenland, together with stepwise combustion isotopic investigation of carbon and nitrogen for the apatite-bearing quartz-magnetite BIF of uncontested sedimentary origin from northeastern ISB.

Ion microprobe analyses reveal that apatites in psammitic schist from the ISB show a U-Pb isochron of 1.5 ± 0.3 Ga. This age is similar to those of Akilia apatite and the Rb-Sr age of 1.6 Ga for the pegmatitic gneiss in the Isukasia area in literature, suggesting a late (~1.5 Ga) metamorphic event (≥400°C). Pb isotopic ratios of apatite in the quartz-magnetite BIF are also affected by the late metamorphic event around 1.5 Ga. Chondrite-normalized REE patterns of apatites in the BIF show flat patterns with a significant positive Eu anomaly, suggesting hydrothermal influence; this is consistent with a primary depositional origin. In contrast with the quartz-magnetite BIF, apatites in the psammitic schist from the ISB and those in the Akilia BIF show different REE patterns, which resemble those of apatites from secondary mafic and felsic rocks, respectively.

Carbon isotopic ratios for the quartz-magnetite BIF by stepwise combustion suggest that two components of reduced carbon are present. One is released below 1000°C (mainly 200–400°C; low-temperature carbon = LTC), and the other above 1000°C (high-temperature carbon = HTC). $\delta^{13}C$ values of the LTC are about –24‰. The LTC is clearly contaminant incorporated after metamorphism, because such a low-temperature component could not have survived the ≥400°C metamorphic event. On the other hand, $\delta^{13}C$ values of the HTC are –30‰ for one aliquot and –19‰ for another. The HTC is probably sequestered within magnetite in the BIF, because the decrepitation temperature of magnetite is ~1200°C. The HTC could not exist within quartz and apatite (decrepitation temperatures: 400–600°C and 600–800°C, respectively), or along grain boundaries. Because the magnetite is concordant with bedding surfaces, it is plausible that the HTC was incorporated in the magnetite during diagenesis. Thus, HTC is the most important candidate for primary carbon

[1]Corresponding author; email: nishizawa@ori.u-tokyo.ac.jp

preserved in the BIF. $\delta^{13}C$ values of HTC cannot be explained as those of Isua carbonate. On the other hand,that the very low $\delta^{13}C$ values (–30‰), negative $\delta^{15}N$ values (–3‰), and low C/N elemental ratios (86) for the >1000°C fraction of one aliquot are comparable to those of kerogen in Archean metasediments. Therefore, despite the presence of secondary carbon (i.e., LTC), the BIF is suggested to possibly contain highly ^{13}C-depleted kerogenous material, which is unlikely to have been incorporated after metamorphism. Although carbon isotopic change of the kerogenous material due to metamorphic effects cannot be precisely determined from the present data, this study shows that further analysis of magnetite from the Isua BIF is a key to the search for the early life.

Introduction

THE OLDEST METASEDIMENTS exposed in the ~3.8 Ga Isua supracrustal belt (ISB) and >3.8 Ga Akilia Island, West Greenland, have been intensively studied to search for the oldest trace of life on Earth (e.g., Schidlowski et al., 1979; Mojzsis et al., 1996; Rosing, 1999). Although the severe metamorphism and deformation would not allow preservation of microfossil structures, ^{13}C-depleted graphite occurs in these oldest metasediments (–50 to –6‰; Oehler and Smith, 1977; Perry and Ahmad, 1977; Schidlowski et al., 1979; Hayes et al., 1983; Shimoyama and Matsubaya, 1992; Naraoka et al., 1996; Mojzsis et al., 1996; Rosing, 1999; Ueno et al., 2002), some of which have comparable $\delta^{13}C$ values to those of biologically produced sedimentary organic carbon of the present Earth. Among these graphites, the most ^{13}C-depleted ones are enclosed within apatite (–20 to –50‰; Mojzsis et al., 1996); thus the apatite-graphite association is a candidate for biomarker. Recently, this idea was challenged by the observations of Fedo and Whitehouse (2002a) and Lepland et al. (2002), suggesting that graphite-bearing apatite occurs only in metasomatized mafic/ultramafic volcanic rocks, whereas apatite in quartz-magnetite BIF of uncontested sedimentary origin is graphite-free. This indicates that some apatites as well as the graphite inclusions would have been incorporated during the metasomatism or metamorphism, thus not of primary depositional origin. Therefore, understanding the geochemistry and geochronology of the apatite is necessary to evaluate the origin and age of the apatite.

Here we report results of *in situ* analyses of rare-earth elements (REEs) of apatites from two metasediments of different lithologies (i.e., quartz-magnetite BIF, and psammitic schist) in the ISB to evaluate the origin of these apatites. The REE pattern of apatite may be used to infer the crystallization environments (Gromlet and Silver, 1983), the chemistry of fluids related to sedimentary environments (Elisabeth and Alain, 1986; Toyoda and Tokonami, 1990), and the effects of metamorphism (Bingen et al., 1996). In addition, results of ion microprobe U-Pb geochronological study of these apatites are also reported, in order to search for primary apatite deposited at ~3.8 Ga. Results of this study suggest that apatites in the quartz-magnetite BIF are of primary depositional origin.

Another question is where ^{13}C-depleted graphite exists in the BIF. Unfortunately, the apatite of our study does not contain visible graphite (>0.1 μm) under the optical microscope. Despite thorough observations of more than 300 thin sections (Ueno et al., 2002; Lepland et al., 2002), graphite has not yet been reported from quartz-magnetite BIF in the ISB. Thus, petrographic study is not always useful to locate the site of ^{13}C-depleted graphite, as demonstrated for Isua turbidite by Rosing (1999). However, this does not prove the absence of graphite in the BIF, because smaller graphite particles and/or inclusions within opaque minerals such as magnetite possibly exist in the BIF. In order to identify the site of the graphite, extraction of carbon was conducted from the sample by stepwise combustion, because graphites enclosed within different minerals are expected to be degassed at distinctive temperature steps. The method has also potential to separate original carbon from secondary contaminant (e.g. Pinti et al., 2001). Recently, Van Zuilen et al. (2002) reported that the reduced carbon in Isua metasediment is almost all released below 500°C, suggesting a post-metamorphic origin. They concluded that there is no evidence for the existence of original reduced carbon in the Isua metasediments. However, carbon isotopic measurements of the higher-temperature fraction (>1000°C) has not been performed so far, and has potential to obtain the original signature. In addition to carbon, measurement of nitrogen is important, because nitrogen is also a bio-essential element.

We also report the results of stepwise combustion measurements for carbon and nitrogen over a wide range of temperature steps (200°–1200°C) for the quartz-magnetite BIF. Based on the release patterns

and their isotopic ratios, we evaluate the site and phase of carbon and nitrogen released at various temperature steps, and discuss timing of their incorporation in the rock and their origin.

Sample and Analytical Method

Sample description

The ~3.8 Ga Isua supracrustal belt (ISB) of West Greenland is the oldest known succession of volcanic and sedimentary rocks on Earth (Nutman, 1986; Appel et al., 1998; Komiya et al., 1999; Myers, 2001; Nutman et al., 2002). Supracrustal rocks are exposed in about a 35 km long arcuate belt (Fig. 1). Most of the rocks underwent metamorphism up to amphibolite facies (e.g., Boak and Dymek, 1982; Nutman, 1986; Hayashi et al., 2000; Appel et al., 2001; Komiya et al., 2002), deformation (e.g., Appel et al., 1998; Myers, 2001; Nutman et al., 2002), and metasomatism (Rose et al., 1996; Rosing et al., 1996), which makes recognition of the protoliths difficult. However, in the northeastern part of the ISB (nearly the same area as the low-strain domain of Appel et al., 1998), primary volcanic and sedimentary structures including pillow lava, pillow breccia, graded bedding, and polymictic conglomerate (Nutman, 1986; Appel et al., 1998; Komiya et al., 1999; Fedo, 2000; Myers, 2001) are exceptionally well preserved. Recently, Appel et al. (2001) reported quartz globules with primary fluid inclusions derived from the ~3.8 Ga hydrothermal metamorphism in the low-strain domain, because the deformation and metasomatism of the domain are relatively weak. Thus, for analyses, we chose two apatite-bearing metasediments from the northeastern ISB.

One sample is quartz-magnetite BIF (43-44A) of uncontested sedimentary origin from the northeastern end of the ISB (Fig. 1). About 20 m thick BIF overlies basaltic pillow lava, and is overlain by bedded chert. Detailed field occurrence of the BIF is also given in Figure 9B of Komiya et al. (1999). The BIF (43-44A) mainly consists of alternating quartz and magnetite layers, with minor amounts of apatite and actinolite (Fig. 2). The apatites are concentrated in a thin (<1 mm) layer, which is concordant with the original bedding surface. Note that under the microscope (>0.1 μm) graphite is not visible in the specimen.

Apatite-bearing psammitic schist (K485) from the northeastern ISB was also selected for analysis (Fig. 1). The sample mainly consists of quartz, with minor amounts of actinolite, anthophyllite, and calcite. Trace amounts of pyrrhotite, chalcopyrite, magnetite, and graphite are also present. Graphite particles occur on grain boundaries of quartz, and occur within mineral such as quartz and garnet. Detailed descriptions are given in Ueno et al. (2002).

For comparison, apatite in the granulite-facies BIF from Akilia Island (Mojzsis et al., 1996; provided by A. P. Nutman) was also studied. ^{13}C-depleted graphite in the apatite of the sample has been claimed as the oldest trace of life (Mojzsis et al., 1996). However, recent field observations and trace element geochemistry by Fedo and Whitehouse (2002a) suggested the possibility that "the Akilia BIF" of Mojzsis et al. (1996) is metasomatized volcanic rock, and the protolith of the rock is still debated (e.g., Fedo and Whitehouse, 2002b; Friend et al., 2002; Mojzsis and Harrison, 2002; Mojzsis et al., 2003; Bolhar et al., 2004). The U-Pb age of 1.5 Ga for the Akilia apatite was reported by Sano et al. (1999b).

Analytical techniques

For ion microprobe analysis, sample chips were cast into epoxy-resin disks with several grains of standard apatite, and polished until mid-sections were exposed. The samples were evacuated in the sample lock overnight, and introduced into the sample stage of the ion source chamber of the Sensitive High Resolution Ion Micro Probe (SHRIMP) installed at Hiroshima University. A primary beam of about 2.5 nA O_{2-} was focused to sputter an area of 20 μm diameter on individual apatite grains and the positive secondary ions were accelerated at 10 kV. There were no isobaric interferences in the mass range over ^{204}Pb and ^{208}Pb at a mass resolution of 5800. Mercury interference on ^{204}Pb was negligible, which was verified by ^{200}Hg and ^{202}Hg measurements (Sano and Terada, 2002). Concentrations of U, Th, and ^{206}Pb were obtained by the relative intensity of each element to the matrix beam of $^{40}Ca_2{}^{31}P^{16}O_3{}^+$. Experimental details were given in Sano et al. (1999a). Analytical data are presented in Tables 1 and 2, and Figures 3 and 4.

Identical primary beam conditions were adopted in rare-earth element (REE) measurements, while the mass resolution of ion microprobe was enhanced to 9300 at 1% peak height in order to separate oxides of light REEs from heavy REEs in cases where we did not use the energy filtering technique. The magnet was cyclically peak-stepped from mass

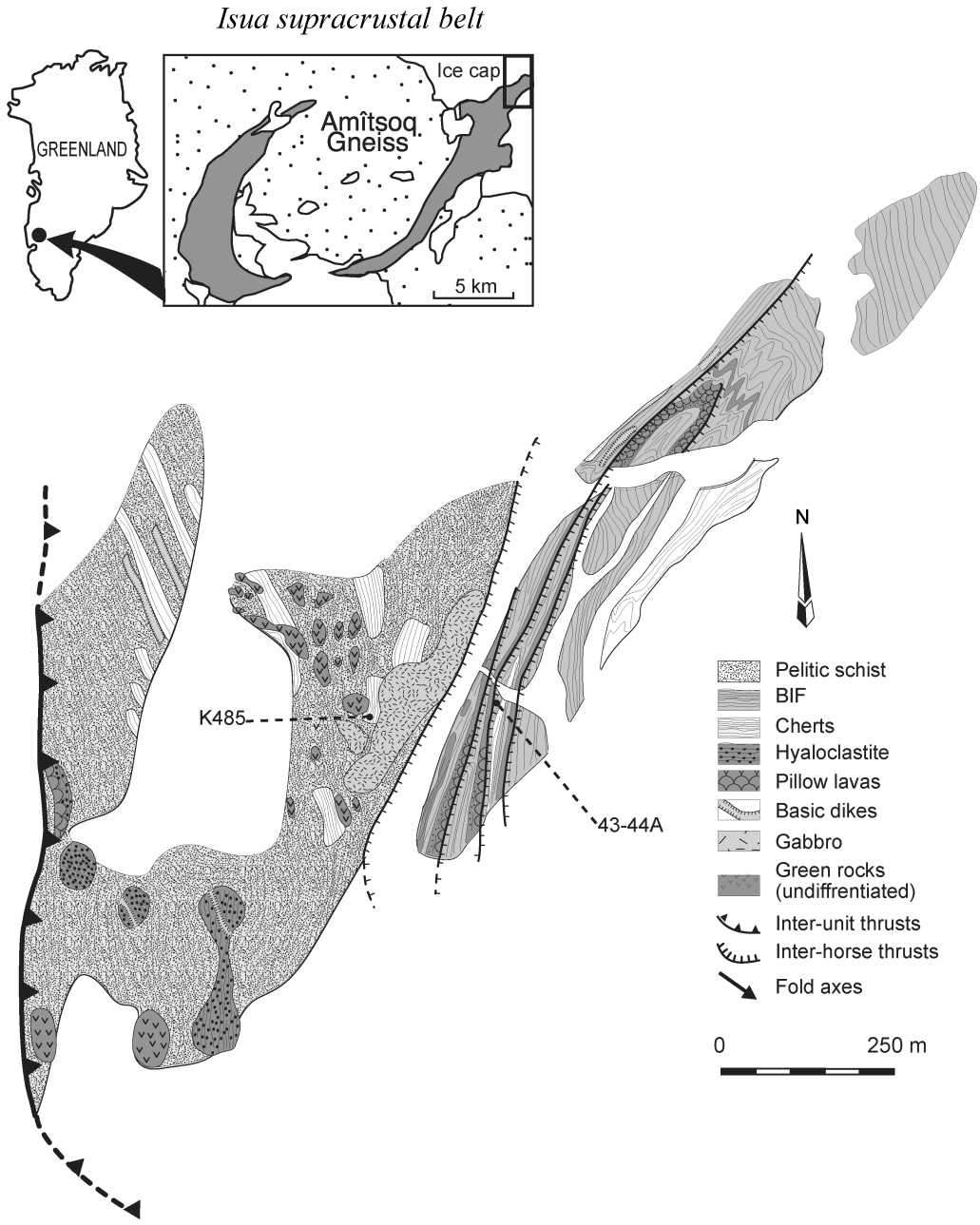

FIG. 1. Geological map of the Isua supracrustal belt, West Greenland (modified after Komiya et al., 1999) showing sample locations.

139 ($^{139}La^+$) to 175 ($^{175}Lu^+$), including the background and all significant REE isotopes ($^{140}Ce^+$, $^{141}Pr^+$, $^{145}Nd^+$, $^{146}Nd^+$, $^{147}Sm^+$, $^{149}Sm^+$, $^{151}Eu^+$, $^{153}Eu^+$, $^{155}Gd^+$, $^{157}Gd^+$, $^{159}Tb^+$, $^{161}Dy^+$, $^{163}Dy^+$, $^{165}Ho^+$, $^{166}Er^+$, $^{167}Er^+$, $^{169}Tm^+$, $^{171}Yb^+$, and $^{172}Yb^+$) and the matrix peak ($^{40}Ca_2{}^{31}P^{16}O_3{}^+$). Observed ratios of $REE^+/^{40}Ca_2{}^{31}P^{16}O_3{}^+$ were calibrated against those of standard apatite, whose REE

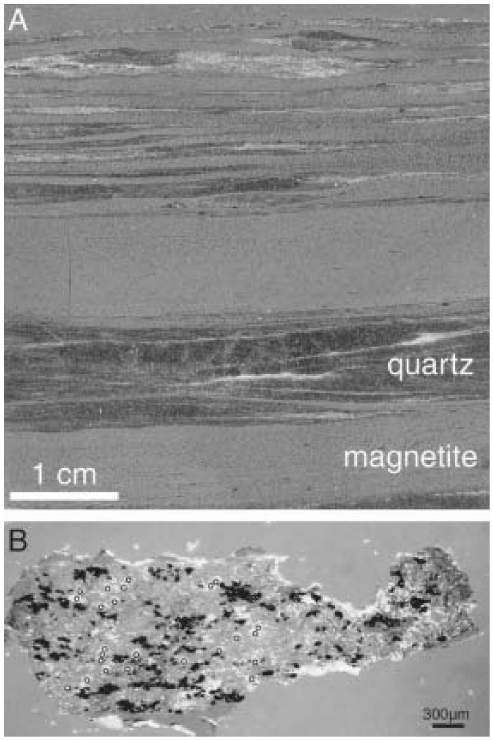

FIG. 2. A. Cut-surface of apatite-bearing quartz-magnetite BIF (43-44A) from the northeastern ISB. Vertical to original bedding surface. Scale bar represents 1 cm. B. Photograph of apatite-rich layer separated from the BIF and mounted on epoxy resin for microprobe analyses. Open circles indicate spots analyzed by SHRIMP. Scale bar represents 300 μm.

abundances were determined by ICP-MS after chemical dissolution (Sano et al., 2002). Analytical data are presented in Table 3 and Figure 5.

For stepwise combustion experiments of BIF 43-44A, the samples were cut into tips (~125 mm^3) by a water-cooled saw. The rock tips contain both quartz and magnetite layers. The tips were ultrasonically washed with distilled water and subsequently acetone, then loaded into a vacuum vessel and baked under vacuum at 200°C for ~8 hours before the measurements. The combustion was carried out in steps of 200°C in order to degas carbon, nitrogen, and argon phases included in quartz, apatite, and magnetite separately. At each step, using two hot copper oxides, two hot platinum foils, and four cryogenic traps, nitrogen and argon were separated, purified from carbonaceous (hydrocarbon, CO_2) gas. The carbonaceous gas was converted to CO_2, then purified and trapped in Pyrex glass tube by traps held at iced pentane and liquid nitrogen temperatures, respectively. Each CO_2-filled tube was cut and sealed by standard glass-blowing techniques. Nitrogen isotopic ratios were measured using a modified noble gas mass spectrometer (VG3600, VG Isotopes Co.) at the Ocean Research Institute, University of Tokyo, by static operation mode. Prior to isotopic analysis, the amount of nitrogen was adjusted to that of air standard gas (0.3–0.6 nmol) in order to compensate for any pressure effect on the isotopic ratio. Experimental details such as abundance measurements of carbon, nitrogen, and argon gases, and blank correction were given by Takahata et al. (1998). Carbon isotopic ratios of the purified CO_2 were measured by a conventional stable isotope mass spectrometer (Finnigan MAT delta S) at Shimane University. Isotopic ratios are reported relative to PDB for carbon and relative to atmospheric N_2 for nitrogen. Analytical data are presented in Table 4 and Figure 6.

Results and Discussion

Rare-earth element abundance in apatite

Table 3 lists concentrations of rare-earth elements for the apatite in the quartz-magnetite BIF (43-44A), the psammitic schist (K485) from ISB, and the Akilia BIF, together with Eu anomalies expressed as Eu/Eu*. Figure 5 shows chondrite-normalized REE patterns for these apatites. Akilia apatite shows a pattern of LREE enrichment and a small positive Eu anomaly. On the other hand, apatite in the psammitic schist (K485) shows a LREE-depleted REE pattern. Apatite in the quartz-magnetite BIF shows a flat pattern with a significant positive Eu anomaly.

The REE pattern of the Akilia apatite is similar to those of apatite in granodiorite from the eastern Peninsular Ranges batholith (Gromlet and Silver, 1983), suggesting that the Akilia apatite was derived from felsic igneous magma (i.e., detrital origin). The REE pattern of the apatite in the psammitic schist (K485) is similar to that of apatite in a mafic dike from the ISB (AL1-2 of Lepland et al., 2002), suggesting that this apatite was derived from mafic igneous magma (i.e. detrital origin).

The REE pattern of apatite in the quartz-magnetite BIF (43-44A) is different from that of secondary apatite in carbonate rocks and mafic dikes from the ISB (i.e., a MREE-enriched convex pattern without

TABLE 1. U and Th Contents, $^{238}U/^{204}Pb$ Ratios, and Pb Isotopic Compositions of Apatite in Psammitic Schist (K485) from the ISB[1]

	U, ppm	Th, ppm	$^{238}U/^{204}Pb$	$^{206}Pb/^{204}Pb$	$^{207}Pb/^{206}Pb$
K485.a	32.9	13.6	194.7 ± 61.2	69.7 ± 19.4	0.367 ± 0.022
K485.b	2.0	4.5	15.5 ± 3.9	24.6 ± 3.3	0.758 ± 0.060
K485.c	1.9	2.3	47.8 ± 17.0	26.9 ± 5.8	0.621 ± 0.047
K485.d	2.2	15.1	29.6 ± 7.8	27.2 ± 6.1	0.708 ± 0.040
K485.e	3.5	17.8	76.5 ± 27.7	36.9 ± 10.2	0.728 ± 0.070
K485.f	1.9	10.7	28.6 ± 7.8	33.5 ± 8.2	0.779 ± 0.045
K485.g	35.5	30.5	410.3 ± 112.7	123.7 ± 30.9	0.240 ± 0.011
K485.h	55.0	56.4	666.0 ± 152.3	212.8 ± 35.9	0.155 ± 0.011
K485.i	3.8	11.2	131.6 ± 44.6	55.6 ± 21.5	0.487 ± 0.093
K485.j	4.9	1.2	149.7 ± 55.5	64.3 ± 23.4	0.341 ± 0.046
K485.k	18.9	12.6	34.2 ± 4.6	23.7 ± 2.7	0.622 ± 0.051

[1]Uncertainty associated with the ratios is 1 sigma. Those of U and Th contents are ± 30% as estimated by repeat measurements of apatite standard.

a Eu anomaly and a LREE-depleted pattern without a positive Eu anomaly, respectively; Lepland et al., 2002). On the other hand, this pattern is similar to that of primary apatite in adjacent BIF from ISB (a flat pattern with a significant positive Eu anomaly; Lepland et al., 2002). A positive Eu anomaly was also measured for quartz-magnetite BIF from the northeastern ISB (Shimizu et al., 1990; Dymek and Klein, 1988). Their REE patterns with positive Eu anomalies suggest that they were likely deposited from hydrothermally influenced contemporaneous seawater. This is because positive Eu anomalies currently are observed for hydrothermal fluids such as at the East Pacific Rise and the Mid-Atlantic Ridge (Eric et al., 1999) and REE characteristics of apatite and BIF are thought to contain signatures of the solution from which they precipitated (Elisabeth and Alain, 1986; Toyoda and Tokonami, 1990; Derry and Jacobsen, 1990). Recently, Appel et al. (2001) showed that metabasites in the Isua supracrustal belt underwent hydrothermal metamorphism at ~3.8 Ga. Therefore, the REE pattern suggests that apatite in the quartz-magnetite BIF was likely deposited from hydrothermally influenced early Archean seawater. This is consistent with a primary depositional origin.

U-Pb dating of apatite

Apatite in psammitic schist (K485). Table 1 lists results of ion microprobe U-Pb dating of apatite separated from the psammitic schist (K485). Figure 3 shows a positive correlation between $^{238}U/^{204}Pb$ and $^{206}Pb/^{204}Pb$ ratios. A least-squares fitting using the York method (York, 1969) yields a ^{238}U-^{206}Pb isochron age of 1533 ± 260 Ma (95% confidence level, MSWD = 0.8, error correlation = 0.789). This age is much younger than the sedimentary age of ~3.8 Ga (Nutman et al., 1997). This suggests that the U-Pb system of apatite in K485 was open at about 1.5 Ga. This age is comparable with a ~1.5 Ga apatite in the Akilia BIF of Mojzsis et al. (1996), dated by Sano et al. (1999b). It is well documented that the Isua supracrustal rocks and the Amîtsoq gneiss were subjected to a series of metamorphic processes (Pankhurst et al., 1973). The most recent thermal event, as suggested by Rb-Sr systematics of muscovite-phengite samples from pegmatitic gneiss in the Isukasia area, was at 1623 ± 65 Ma (Baadsgaard et al., 1986), which may have a close relation with the ~1.5 Ga apatite.

Using Dodson's (1973) equation, an activation energy of 229 kJ/mol, and a frequency factor of 2×10^{-8} m^2/sec (Cherniak et al., 1991), the closure

TABLE 2. U, Th, and Pb contents, and Pb Isotopic Compositions of Apatite in Quartz-Magnetite BIF (43-44A) from the ISB[1]

Sample	U, ppm	Th, ppm	^{206}Pb, ppm	$^{206}Pb/^{204}Pb$	$^{207}Pb/^{204}Pb$	$^{208}Pb/^{204}Pb$
43-44A.420.a	0.020	0.004	0.98	13.12 ± 0.22	13.66 ± 0.38	32.97 ± 0.78
43-44A.420.b				12.53 ± 0.24	13.88 ± 0.31	32.19 ± 0.84
43-44A.420.c				13.13 ± 0.33	13.46 ± 0.44	31.83 ± 1.08
43-44A.420.d				13.63 ± 0.27	14.60 ± 0.35	34.74 ± 0.94
43-44A.420.e				12.87 ± 0.38	14.19 ± 0.47	32.05 ± 1.49
43-44A.420.f	0.051	0.020	1.24	12.06 ± 0.19	13.02 ± 0.28	30.33 ± 0.87
43-44A.420.g				11.58 ± 0.44	12.78 ± 0.82	29.87 ± 1.75
43-44A.420.h				12.48 ± 0.28	12.70 ± 0.40	30.74 ± 1.12
43-44A.420.i				12.91 ± 0.27	13.68 ± 0.33	31.68 ± 0.88
43-44A.420.j				13.04 ± 0.37	14.17 ± 0.47	33.56 ± 1.26
43-44A.420.k				12.35 ± 0.36	13.16 ± 0.46	32.15 ± 1.33
43-44A.420.l				12.94 ± 0.27	14.19 ± 0.42	32.91 ± 1.15
43-44A.420.m				12.01 ± 0.23	13.34 ± 0.30	31.02 ± 0.92
43-44A.420.n	0.072	0.033	2.88	13.85 ± 0.11	14.56 ± 0.33	34.90 ± 0.68
43-44A.420.o				12.29 ± 0.12	13.29 ± 0.25	30.72 ± 0.54
43-44A.420.p				11.81 ± 0.14	13.04 ± 0.24	30.50 ± 0.66
43-44A.420.q				12.16 ± 0.27	13.72 ± 0.82	32.35 ± 1.78
43-44A.420.r				11.55 ± 0.19	13.21 ± 0.40	31.07 ± 1.80
43-44A.420.s				12.12 ± 0.23	14.02 ± 0.69	32.67 ± 1.31
43-44A.420.t				14.06 ± 0.29	14.03 ± 0.45	32.62 ± 1.23
43-44A.420.u				16.40 ± 0.48	15.33 ± 0.68	36.88 ± 1.79
43-44A.420.v	0.057	0.019	1.80	12.19 ± 0.15	13.18 ± 0.24	30.52 ± 0.70
43-44A.420.w				12.00 ± 0.20	13.73 ± 0.80	33.06 ± 1.60
43-44A.420.x				12.53 ± 0.57	13.80 ± 1.26	32.98 ± 2.20
Average	0.050	0.019	1.72	12.61 ± 0.04	13.56 ± 0.08	31.98 ± 0.20

[1]Uncertainty associated with the ratios is 1 sigma. Those of contents are ± 30%. Because contents of U and Th were very low, measurements were carried out for 4 spots.

temperature is estimated to be 384–419°C for the apatite U-Pb system with a 30 μm grain size and at a slow cooling rate of 1–10°C/Ma. The estimate suggests that the K485 underwent metamorphism above 400°C at 1.5 Ga.

Apatite in quartz-magnetite BIF (43-44A). Table 2 lists U, ^{206}Pb concentrations, and Pb isotopic ratios of the apatite in the quartz-magnetite BIF (43-44A). Inasmuch as U contents are substantially lower than Pb contents, *in situ* radiogenic production of ^{206}Pb and ^{207}Pb during geological time is suggested to have been negligibly small, probably within the analytical uncertainty of the observed Pb isotopic ratio at the 2σ level. We compared the Pb isotopic ratios of the apatite in the BIF with two Pb growth models (Fig. 4). One is the model for

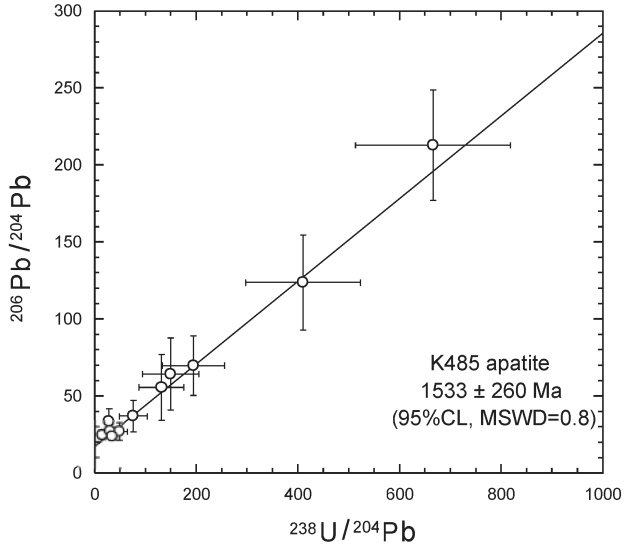

FIG. 3. Correlation diagram of $^{238}U/^{204}Pb$–$^{206}Pb/^{204}Pb$ ratios of apatite in psammitic schist (K485) from ISB. Uncertainty associated with the ratios is 1 sigma. Solid line is the best fit using the York method (York, 1969). In the fitting calculation, we take error correlation of Rec = 0.872, which is calculated by the correlation coefficient between $\delta(^{238}U/^{204}Pb)/(^{238}U/^{204}Pb)$ and $\delta(^{206}Pb/^{204}Pb)/(^{206}Pb/^{204}Pb)$.

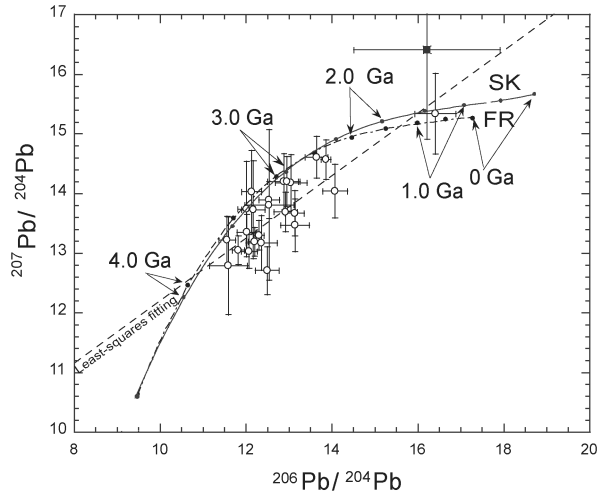

FIG. 4. Pb isotopic ratios of apatite (open circles) in quartz-magnetite BIF (43-44A) from northeastern ISB. Uncertainty assigned to the ratios is 1 sigma. A black square indicates the initial Pb isotopic ratio of the ~1.5 Ga apatite in K485, for comparison. Two model growth curves for terrestrial Pb (SK = Stacey and Kramers, 1975) and Early Archean Pb (FR = Frei and Rosing, 2001) are also shown. Using the York (1969) method, best fit of the Pb isotopic ratios of the apatite (43-44A) intersects the growth curves at model Pb ages of 3.9 ± 0.2 and 1.5 (+0.6, –1.1) Ga for the SK model, and at 4.0 ± 0.2 and 1.2 (+ 0.6, –1.2) Ga for the FR model, respectively.

terrestrial Pb (Stacey and Kramers, 1975; named SK model), and the other for Early Archean Pb defined by galena from the western part of ISB (Frei and Rosing, 2001; named FR model). Figure 4 also shows the initial Pb isotopic ratio of the apatite in adjacent psammitic schist (K485), which is

TABLE 3. Rare-Earth Element Abundances (ppm) of Apatites from ISB and Akilia Island, West Greenland[1]

	43-44A.420.y	43-44A.421.a	K485.l	K485.m	Akilia.a	Akilia.b
La	5.0	3.7	5.1	6.5	495.0	456.0
Ce	31.0	19.7	27.6	26.6	1030.0	870.0
Pr	5.0	3.9	5.5	4.7	89.5	80.0
Nd	21.2	19.9	23.3	22.2	330.0	285.0
Sm	7.2	7.1	8.0	7.3	58.0	50.5
Eu	6.5	6.3	5.6	4.9	25.7	24.0
Gd	9.2	10.1	27.6	24.1	79.6	64.1
Tb	1.6	1.7	8.6	7.2	12.2	10.4
Dy	8.9	10.0	48.8	43.1	63.6	55.7
Ho	2.1	2.4	11.2	9.1	13.6	11.5
Er	7.1	7.1	28.4	26.8	37.1	29.9
Tm	1.2	1.2	4.1	3.8	4.8	3.6
Yb	8.5	8.7	18.4	16.6	24.2	17.9
Lu	1.5	1.6	3.1	2.9	3.7	3.5
sum REE	120.0	100.0	225.0	206.0	2270.0	1960.0
$(Eu/Eu^*)_{CN}$	2.4	2.3	1.2	1.1	1.1	1.3

[1]Uncertainty in REE abundances is ± 20% based on repeat measurements of apatite standard. $(Eu/Eu^*)_{CN} = (Eu)_{CN}/\{(Sm)_{CN}*(Gd_{CN})\}^{0.5}$; CN means chondrite normalization.

calculated by a 3D linear regression for the total U/Pb isochron, constrained to intersect the Tera-Wasserburg concordia (Ludwig, 1998).

As shown in Figure 4, the apatite in the BIF has various Pb isotopic ratios. Within analytical uncertainty, one of the data points corresponds to the initial Pb isotopic ratio for apatite in K485 with a ~1.5 Ga U-Pb age, suggesting incorporation of Pb derived from the ~1.5 Ga metamorphism. However, most of the other data points are scattered toward ~3.8 Ga. This may indicate a two-component mixing trend. Least-squares fitting for the Pb isotopic ratios of the apatite by York (1969) method gives a slope of 0.52 ± 0.15 and a Y-intercept of 7.0 ± 1.9 (95% confidence level, MSWD = 1.3, error correlation = 0.742). The fitting line has two intersects with the Pb growth curve at model Pb ages of 3.9 ± 0.2 and 1.5 (+0.6, –1.1) Ga for SK model, and at 4.0 ± 0.2 and 1.2 (+0.6, –1.2) Ga for FR model. The older model Pb age of the intersection is consistent with depositional age of the BIF (Nutman et al., 1997), even though either model is adopted.

Because the quartz-magnetite BIF contains extremely unradiogenic Pb (Moorbath et al., 1973; Frei et al., 1999), it cannot be ruled out that apatite incorporated ancient Pb from the BIF during metamorphic event(s) above 400°C. In this case, the older model age is not a direct estimate of age of the apatite, but corresponds to the age of the BIF (43-44A). On the other hand, the REE pattern of the apatite suggests that the apatite had a primary and hydrothermal depositional origin, as discussed in the previous section. This is consistent with the fact that closure temperature of REE in apatite is much higher than that of Pb; a closure temperature for Nd is 612–655°C, whereas that for Pb is 384–419°C for apatite with a 30 μm grain size at a cooling rate of 1–10°C/Ma; (Cherniak et al., 1991; Cherniak 2000). Therefore, the apatite was also formed at ~3.8 Ga even in the latter case, because the formation of

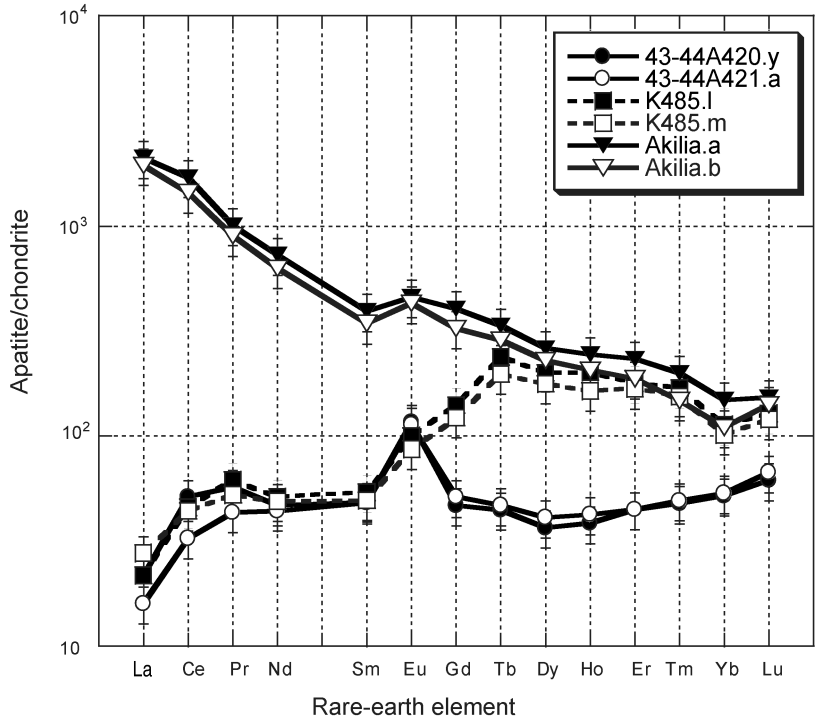

FIG. 5. Chondrite-normalized rare-earth element abundance patterns of apatites in the quartz-magnetite BIF (43-44A) and psammitic schist (K485) from the ISB. Data for graphite-bearing apatites in granulite-facies BIF from the Akilia Island (Mojzsis et al., 1996) are also shown. Uncertainty assigned to the abundance is 1 sigma.

apatite is simultaneous with the deposition of the BIF. Thus, it is important to locate the carbon and nitrogen within the primary apatite in the BIF. In the following sections, we discuss the site (e.g., within apatite, magnetite), age, and the origin of carbon and nitrogen in the BIF, based on results of stepwise combustion of the BIF.

Stepwise combustion experiments of carbon and nitrogen for 43-44A BIF

For the quartz-magnetite BIF (43-44A) from the northeastern ISB, carbon and nitrogen isotopic ratios were measured by stepwise combustion. Contents, isotopic and elemental ratios of carbon and nitrogen released from each temperature step are shown in Table 4. Figure 6 shows release patterns of two aliquots from the same BIF. Carbon and nitrogen abundances show two major peaks, with distinctive isotopic ratios. For carbon, two major peaks are identified at temperature steps of 200–400°C and 1000–1200°C, whereas for nitrogen, two peaks appear at steps of 400–600°C and 1000–1200°C. In the following section, we discuss two groups of released gases, separately. One is released below 1000°C, and the other above 1000°C.

Carbon and nitrogen released at temperature below 1000°C. Below 1000°C, there are abundance peaks at a step of 200–400°C for carbon, and 400–600°C for nitrogen. The $\delta^{13}C$ values of the peak fractions are –23.55 ± 0.02‰ for one aliquot (4c), and –25.08 ± 0.03‰ for another (5c), whereas the $\delta^{15}N$ value is +6.9 ± 0.8 and +1.7 ± 0.6‰ for 4c and 5c, respectively.

The carbon released below 400°C probably is a secondary contaminant incorporated after metamorphism, because the BIF probably experienced ~400°C metamorphism (Hayashi et al., 2000). Such a low-temperature fraction is unlikely to have survived the metamorphic events. The carbon released below 400°C probably exists along grain boundaries, because decrepitation temperatures of quartz (400–600°C; Sano and Pillinger, 1990), apatite (600–800°C; Nadeau et al., 1999), and magnetite (~1200°C; Tolstikhin et al., 2002), which are the

TABLE 4. Summary of Stepwise Combustion Experiments, Showing N and C Contents, C/N Atomic Ratios, and N and C Isotopic Compositions of the Quartz-Magnetite BIF (43-44A) from the ISB[1]

Temp. °C	N ppm	C ppm	C/N atomic ratio	$\delta^{15}N$ ‰	$\delta^{13}C$ ‰
			4c, 300.6 mg		
200	–	3.9	–	–	–
400	0.056	33.0	688	2.6 ± 0.6	–23.55 ± 0.02
600	0.210	12.0	67	6.9 ± 0.8	–24.03 ± 0.03
800	0.075	3.5	54	11.4 ± 0.6	–
1000	0.030	6.8	264	7.8 ± 0.8	–20.73 ± 0.04
1200	0.019	11.0	675	0.8 ± 7.4	–18.82 ± 0.02
Total	0.390	70.2	210	6.9	–21.3
			5c, 288.2 mg		
200	–	2.1	–	–	–
400	0.122	20.0	191	–0.2 ± 0.6	–25.08 ± 0.03
600	0.419	14.0	39	1.7 ± 0.6	–25.31 ± 0.02
800	0.110	2.0	21	7.1 ± 0.6	–
1000	0.054	2.5	54	5.3 ± 0.6	–
1200	0.258	19.0	86	–3.1 ± 0.7	–30.25 ± 0.02
Total	0.963	59.6	72	1.0	–27.0

[1]Uncertainty assigned to $\delta^{15}N$ values and $\delta^{13}C$ values are 1 sigma; " – " = blank level or below detection limit.

main components of the BIF (43-44A), are higher than 400°C; thus the low-temperature fraction is not expected to be released from these minerals. $\delta^{13}C$ values of the carbon released below 400°C (–23 to –25‰) are similar to those of sedimentary organic carbon on the present Earth, but are different from Isua carbonates (–7 to +5‰; Oehler and Smith, 1977; Perry and Ahmad, 1977; Schidlowski et al., 1979). Thus, secondary reduced carbon probably exists along grain boundaries of the BIF. This result indicates that we should be careful to identify and separate potential primary carbon from the secondary carbon.

In addition, a smaller amount of carbon is released at 400–1000°C. This carbon is possibly derived from inclusions within quartz and apatite, which release their inclusions at these temperature steps. However, we cannot evaluate their contributions to the amount of released carbon because reduced carbon along grain boundaries could also be degassed over a wide range of temperatures below 1000°C, by analogy with the combustion temperature for kerogen (e.g., Wedeking et al., 1983; Beaumont and Robert, 1999).

It is important that no release peak was observed at 600–800°C, which corresponds to the decrepitation temperature of apatite. Thus, there is no evidence to show a close relationship between apatite and ^{13}C-depleted reduced carbon. The presence of apatite does not necessarily mean the existence of a "biomarker".

On the other hand, the phases of nitrogen released at 400–600°C are problematic. One possible phase is N_2-fluid enclosed within quartz. Pinti et al. (2001) also identified nitrogen with $\delta^{15}N$ values of about +7‰ released at ~600°C, associated with a major peak of primordial ^{36}Ar abundance, by stepwise combustion of Isua metacherts. They concluded that the nitrogen was derived from fluid inclusions enclosed in quartz. $\delta^{15}N$ values of our

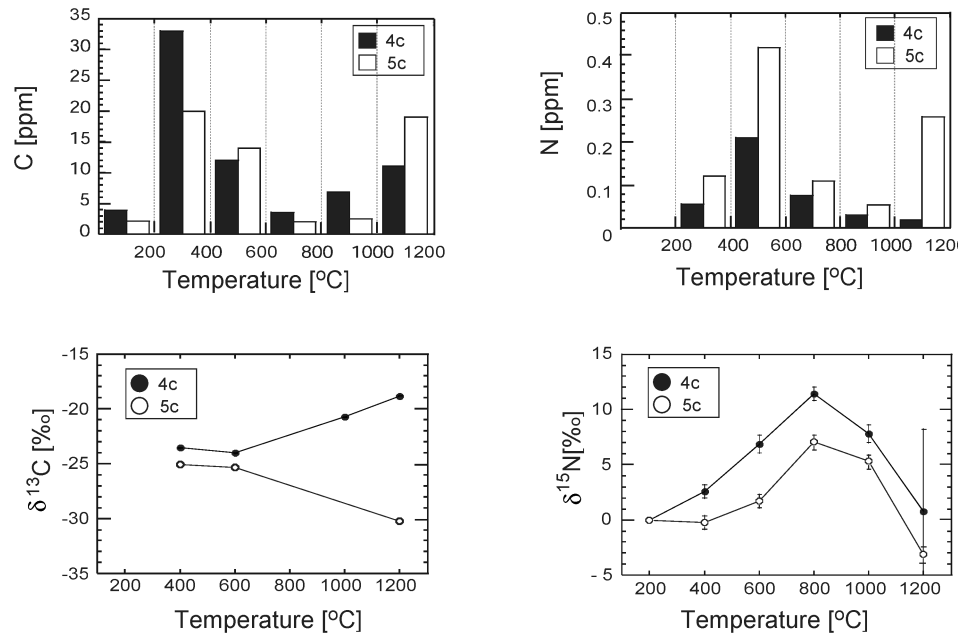

FIG. 6. Results of stepwise combustion experiments for two aliquots (4c and 5c) of the quartz-magnetite BIF (43-44A). Stepwise release patterns of abundances and isotopic ratios of carbon and nitrogen are shown. One sigma error bars are shown for nitrogen isotope ratios. For carbon isotope ratios, one sigma error bars are within the symbol size.

sample 4c (6.9 ± 0.8‰) are closely similar to the fluid nitrogen of Pinti et al. (2001). The other possible phase for the nitrogen is kerogenous material on grain boundaries and/or within quartz.

Carbon and nitrogen released above 1000°C. Above 1000°C, there are release peaks both for carbon and nitrogen (Fig. 6). $\delta^{13}C$ values and $\delta^{15}N$ values are –18.82 ± 0.02‰ and 0.8 ± 7.4‰ for one aliquot (4c), and –30.25 ± 0.02‰, –3.1 ± 0.7‰ for another (5c), respectively. These high-temperature fractions are very important as a candidate for primary organic matter, because their high release temperature makes their post-metamorphic origin unlikely, as discussed in the following sections. We named the carbon and nitrogen released above 1000°C HTC and HTN, respectively. In the following sections, we discuss site, phase, and origin of the HTC and HTN.

Site of HTC and HTN, and the timing of their incorporation into the BIF: The BIF (43-44A) consists mainly of quartz and magnetite with minor apatite and actinolite. Among these minerals, only magnetite has a decrepitation temperature over 1000°C (~1200°C; Tolstikhin et al., 2002), suggesting that HTC exists within the magnetite. In addition, it is unlikely that HTC is on grain boundaries and/or on the sample surface, because the combustion temperature of kerogen is below 1000°C (e.g. Wedeking et al., 1983; Beaumont and Robert, 1999). Thus, HTC probably exists within the magnetite. This idea is also supported by an earlier study which showed that peaks of release abundance of carbon and nitrogen occur above 1000°C by stepwise combustion of magnetite separated from Isua BIF (Pinti et al., 2001). Therefore, the precursors of HTC and HTN were probably present at the time of magnetite formation.

Magnetite of the analyzed specimen occurs along bedding surfaces, and not as secondary veins (Fig. 2). Thus, it is plausible that the HTC and HTN would have been entrapped by magnetite during diagenesis of the quartz-magnetite BIF. In addition, the metamorphic age of bedded magnetite in BIF from the same northeastern end of the ISB is 3.69 Ga, estimated by Pb-Pb systematics (Frei et al., 1999). This indicates that the carbon and nitrogen were incorporated in the BIF before 3.69 Ga.

Phase of HTC and HTN: Possible candidates for the phase of HTC are graphite (including kerogenous material), fluid, and carbonate. The $\delta^{13}C$

values of the HTC are much lower than those of Isua carbonate (–7 to +5‰; Oehler and Smith, 1977; Perry and Ahmad, 1977; Schidlowski et al., 1979), and those of CO_2 gas (likely ≥10‰). Thus, it is unlikely that the HTC was derived from carbonate or CO_2 fluid. Significant ^{13}C depletions of HTC (up to –30‰) suggest that the HTC is derived from graphitic or kerogenous material.

The kerogenous origin of HTC is consistent with the negative $\delta^{15}N$ value of HTN (–3‰) and their C/N ratio (86) for one aliquot (5c), because these values are within the range of those of Archean kerogen in metasediments (Beaumont and Robert, 1999). This suggests that HTN would be derived from kerogenous material. In summary, the phase of HTC and HTN is suggested to be kerogenous material.

Origin of HTC: On the basis of the above discussion, we conclude that ^{13}C-depleted (up to –30‰) kerogenous material exists within magnetite of the quartz-magnetite BIF. In contrast with secondary reduced carbon released mainly below 400°C, the precursor of the HTC would have been incorporated into magnetite during diagenesis. Previous studies reported $\delta^{13}C$ values of ≥–19‰ for graphite of premetamorphic origin from Isua metasediments (Rosing 1999; Ueno et al., 2002). In contrast, this study first suggests that bedded magnetite in BIF from the northeastern end of the ISB contains more ^{13}C-depleted carbon (up to –30‰) of primary origin. Thus, it is important to discuss the origin of HTC as well as HTN to test for early life.

In order to discuss the origin of the HTC, secondary isotope fractionation of the precursor of the HTC during metamorphism was calculated. Attending the stepwise combustion experiments of the BIF, trace amounts of H_2O (ppm) was also detected above 1000°C. Thus, it is possible that the precursor of HTC (kerogenous material) reacted with H_2O in magnetite and lost CO_2- and CH_4-bearing fluid during metamorphism. Secondary isotope fractionation of the precursor of HTC due to loss of CO_2- and CH_4-bearing fluid was estimated employing a Rayleigh distillation model. In the model, we used following equation:

$$\delta^{13}C_{final} - \delta^{13}C_{initial} = (F^{\alpha-1} - 1) \times (\delta^{13}C_{initial} + 1000) \approx (F^{\alpha-1} - 1) \times 1000$$

Values of $\delta^{13}C_{final}$ and $\delta^{13}C_{initial}$ refer to the $\delta^{13}C$ value of kerogenous material after metamorphism and before metamorphism, respectively. F refers to the fraction of kerogenous material remaining, and α is a carbon isotope fractionation factor of the C-bearing fluid relative to the remaining kerogenous material. Detailed explanation of the metamorphic temperature, total fluid pressure, oxygen fugacity, and α value are given in the Appendix.

As shown in Figure 7B, the direction of carbon isotopic change of the kerogenous material during metamorphism depends on the CO_2/CH_4 molar ratio of the fluid (i.e., oxygen fugacity within magnetite). It is possible that the $\delta^{13}C_{initial}$ value was more negative than the $\delta^{13}C_{final}$ value in some cases (i.e., CO_2/CH_4 molar ratio ≤ 0.73 at T = 400°C). Here, the precursor of HTC would have been more ^{13}C-depleted than HTC, and HTC (^{13}C-depleted up to –30‰) is possibly derived from organic carbon produced by early life. On the other hand, it is also possible that the $\delta^{13}C_{initial}$ value is more positive than the $\delta^{13}C_{final}$ value (i.e., CO_2/CH_4 molar ratio > 0.73 at T = 400°C). In these cases, the precursor of HTC would have been more ^{13}C-enriched than HTC, and HTC (^{13}C-depleted up to –30‰) possibly would have been derived from abiological graphite produced by siderite decomposition ($\delta^{13}C$ value of –10 to –12‰; Van Zuilen et al., 2002). For example, the value of $\delta^{13}C_{final} - \delta^{13}C_{initial}$ can be –18‰ when the F value decreases to 0.20, due to loss of pure CO_2 at 400°C.

Although we cannot exclude the possibility of abiological graphite as the origin of the HTC with the present data set, the fact that the HTC and HTN have $\delta^{13}C$ values, $\delta^{15}N$ values, and C/N elemental ratios consistent with Archean kerogen (Beaumont and Robert, 1999) indicates that HTC was not derived from abiological graphite. For precise estimation of the isotopic change of the precursor of HTC and HTN during metamorphism, further study is important to elucidate the relation between content and isotopic ratio of HTC and HTN, respectively.

Conclusions

Ion microprobe REE geochemistry and U-Pb geochronology of apatite in ~3.8 Ga metasediments, together with carbon and nitrogen isotopic analyses of the quartz-magnetite BIF by stepwise combustion, provide the following new information.

1. The chondrite-normalized REE pattern of apatite in the quartz-magnetite BIF (43-44A) is flat with a positive Eu anomaly. This pattern is different from that of secondary apatite in carbonate rocks and

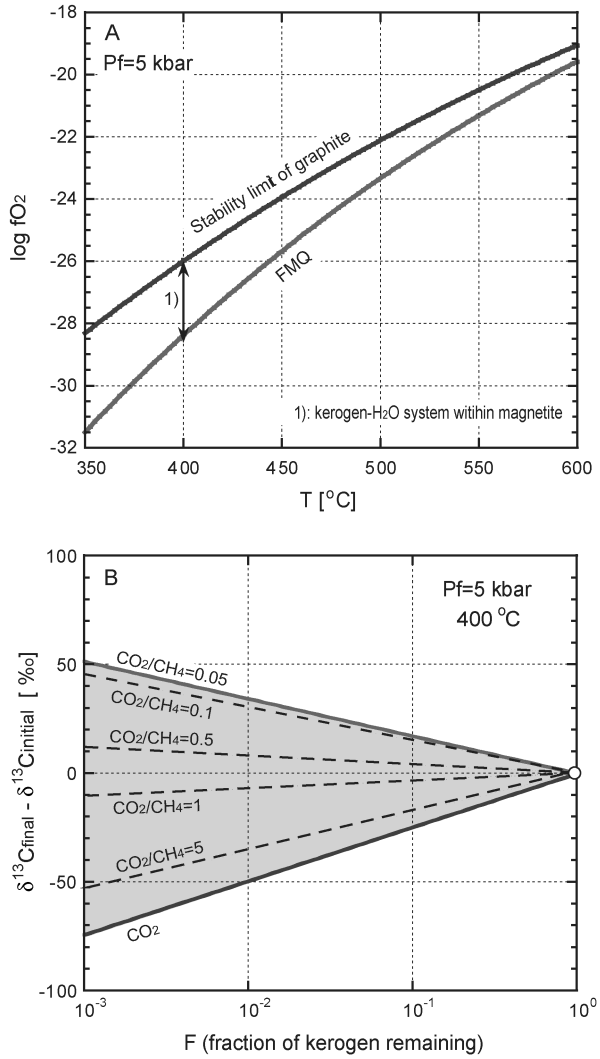

FIG. 7. Calculated change in $\delta^{13}C$ value of precursor of HTC (kerogenous material) due to loss of CO_2- and CH_4-bearing fluid during metamorphism. The precursor of HTC is suggested to have coexisted with H_2O, both within magnetite in BIF 43-44A. Rayleigh distillation model was used for the calculation. A. Relation between oxygen fugacity and metamorphic temperature of the kerogenous material–H_2O system within magnetite in the BIF. We assumed that oxygen fugacity of the kerogenous material–H_2O system is higher than that determined by FMQ buffer and lower than that determined by graphite buffer. B. Calculated change of $\delta^{13}C$ value of the kerogenous material due to loss of CO_2- and CH_4-bearing fluid at 400°C. The range of CO_2/CH_4 molar ratio of the C-bearing fluid was estimated within the range of oxygen fugacity of the kerogenous material–H_2O system determined by Figure 7A.

mafic dikes from the ISB, respectively (Lepland et al., 2002). On the other hand, the REE pattern suggests that the apatite was likely deposited from hydrothermally influenced Early Archean seawater. This is consistent with the primary depositional origin of the apatite and the BIF.

2. Apatite in the quartz-magnetite BIF is U-poor, and records various Pb isotopic ratios, which may be

explained by mixing of two model age components (~3.8 Ga and ~1.5 Ga). This suggests that the quartz-magnetite BIF was affected by metamorphism at 1.5 Ga.

3. Apatite in the psammitic schist (K485) shows a U-Pb isochron of 1.5 ± 0.3 Ga, supporting metamorphism at 1.5 Ga. This age is also consistent with a Rb-Sr age of 1.6 Ga for muscovite-phengite samples from pegmatitic gneiss in the Isukasia area (Baadsgaard et al., 1986).

4. Stepwise combustion experiments suggest that quartz-magnetite BIF (43-44A) contains two distinctive components of carbon. One is released below 1000°C (mostly released between 200° and 400°C); it probably exists along grain boundaries, and is clearly contaminant incorporated after the metamorphism. The other is released above 1000°C, and is probably included in magnetite which occurs concordantly with bedding. Thus, it is plausible that the precursor of the high-temperature carbon was incorporated into magnetite during diagenesis of the BIF (~3.8 Ga).

5. Significant ^{13}C depletion (–30‰), as well as negative $\delta^{15}N$ values (–3‰), and C/N ratios (86) of the high-temperature fraction for one aliquot of the BIF are within the range of those of Archean kerogen in metasediments. This suggests that these elements were derived from kerogenous material.

These lines of evidence indicate that the apatite-bearing quartz-magnetite BIF may preserve a primary depositional signature at ~3.8 Ga. Despite the presence of secondary carbon (i.e., LTC), the BIF is suggested to contain pre-metamorphic ^{13}C-depleted carbon (up to –30‰), entrapped by magnetite during diagenesis.

Acknowledgments

We thank R. Yokochi and T. Monde for analytical assistance; T. K. Dalai for improvement of the English; S. Maruyama and H. Shimizu for discussions; A. P. Nutman and H. Yoshioka for providing sedimentary rock samples; and K. Ludwig for the Isoplot/Ex. computer software. We thank M. T. Rosing for a critical review of an early draft of the manuscript. Constructive review by E. G. Nisbet greatly improved the manuscript. YU is grateful for the Research Fellowships of the Japan Society for the Promotion of Science for Young Scientists. This is a contribution of a joint project between the SHRIMP laboratory at Hiroshima University and the Center for Advanced Marine Research at the Ocean Research Institute, University of Tokyo.

REFERENCES

Appel, P. W. U., Fedo, C. M., Moorbath, S., and Myers, J. S., 1998, Recognizable primary volcanic and sedimentary features in a low-strain domain of the highly deformed, oldest known (~3.7-3.8 Gyr) Greenstone Belt, Isua, West Greenland:. Terra Nova, v. 10, p. 57–62.

Appel, P. W. U., Rollinson, H. R., and Touret, J. L. R., 2001, Remnants of an Early Archaean (>3.75 Ga) seafloor, hydrothermal system in the Isua Greenstone Belt: Precambrian Research, v. 112, p. 27–49.

Baadsgaard, H., Nutman, A. P., Rosing, M., Bridgwater, D., and Longstaffe, F. J., 1986, Alteration and metamorphism of Amitsoq gneisses from the Isukasia area, west Greenland: Recommendations for isotope studies of the early crust: Geochimica et Cosmochimica Acta, v. 50, p. 2165–2172.

Beaumont, V. and Robert, F., 1999, Nitrogen isotope ratios of kerogens in Precambrian cherts: A record of the evolution of atmosphere chemistry: Precambrian Research, v. 96, p. 63–82.

Bingen, B., Demaiffe, D., and Hertogen, J., 1996, Redistribution of rare earth elements, thorium, and uranium over accessory minerals in the course of amphibolite-to granulite-facies metamorphism: The role of apatite and monazite in orthogneisses from southwestern Norway: Geochimica et Cosmochimica Acta, v. 60, p. 1341–1354.

Boak, J. L., and Dymek, R. F., 1982, Metamorphism of the ca. 3800 Ma supracrustal rocks at Isua, West Greenland: Implications for early Archean crustal evolution: Earth And Planetary Science Letters, v. 59, p. 155–176.

Bolhar, R., Kamber, B. S., Moorbath, S., Fedo, C. M., and Whitehouse, M. J., 2004, Characterisation of early Archaean chemical sediments by trace element signatures?: Earth And Planetary Science Letters, v. 222, p. 43–60.

Chacko, T., Mayeda, T. K., Clayton, R. N., and Goldsmith, J. R., 1991, Oxygen and carbon isotope fractionations between CO_2 and calcite: Geochimica et Cosmochimica Acta, v. 55, p. 2867–2882.

Cherniak, D. J., 2000, Rare earth element diffusion in apatite: Geochimica et Cosmochimica Acta, v. 64, p. 3871–3885.

Cherniak, D. J., Lanford, W. A., and Ryerson, F. J., 1991, Lead diffusion in apatite and zircon using ion implantation and Rutherford backscattering techniques: Geochimica et Cosmochimica Acta, v. 55, p. 1663–1673.

Derry, L. A., and Jacobsen, S. B., 1990, The chemical evolution of Precambrian seawater: Evidence from

REEs in banded iron formations: Geochimica et Cosmochimica Acta, v. 54, p. 2965–2977.

Dodson, M. H., 1973, Closure temperature in cooling geochronological and petrological systems: Contributions to Mineralogy and Petrology, v. 40, p. 259–274.

Dymek, R. F. and Klein, C., 1988, Chemistry, petrology and origin of banded iron-formation lithologies from the 3800 Ma Isua supracrustal belt, West Greenland: Precambrian Research, v. 39, p. 247–302.

Dymek, R. F., Brothers, S. C., and Schiffries, C. M., 1988, Petrogenesis of ultramafic metamorphic rocks from the 3800 Ma Isua supracrustal belt, West Greenland. Journal of Petrology, v. 29, p. 1353–1397.

Dodson, M. H., 1973, Closure temperature in cooling geochronological and petrological systems: Contributions to Mineralogy and Petrology, v. 40, p. 259–274.

Elisabeth, O., and Alain, C., 1986, Fish debris record the hydrothermal activity in the Atlantis 2 Deep sediments (Red Sea): Geochimica et Cosmochimica Acta, v. 52, p. 177–184.

Eric, D., Philippe, B., Jean, L. C., Jean, P. D., Yves, F., Pierre, A., and Gamo, T., 1999, Yttrium and rare earth elements in fluids from various deep-sea hydrothermal systems: Geochimica et Cosmochimica Acta, v. 63, p. 627–643.

Fedo, C. M., 2000, Setting and origin for problematic rocks from the >3.7 Ga Isua Greenstone Belt, southern west Greenland: Earth's oldest coarse clastic sediments: Precambrian Research, v. 101, p. 69–78.

Fedo, C. M., and Whitehouse M. J., 2002a, Metasomatic origin of quartz-pyroxene rock, Akilia, Greenland, and implication for Earth's earliest life: Science, v. 296, p. 1448–1452.

Fedo, C. M. and Whitehouse M. J., 2002b, Origin and significance of Archean quartzose rocks at Akilia, Greenland: Response: Science, v. 298, p. 917a.

Friend, C. R. L., Nutman, A. P., and Bennett, V. C., 2002, Origin and significance of Archean quartzose rocks at Akilia, Greenland: Science, v. 298, p. 917a.

Frei, R., Bridgwater, D., Rosing, M., and Stecher, O., 1999, Controversial Pb-Pb and Sm-Nd isotope results in the early Archean Isua (West Greenland) oxide iron formation: Preservation of primary signatures versus secondary disturbances: Geochimica et Cosmochimica Acta, v. 63, p. 473–488.

Frei, R. and Rosing, M. T., 2001, The least radiogenic terrestrial lead; implications for early Archean crustal evolution and hydrothermal-metasomatic processes in the Isua supracrustal belt (West Greenland): Chemical Geology, v. 181, p. 47–66.

Gromlet, L. P., and Silver, L. T., 1983, Rare earth element distributions among minerals in a granodiorite and their petrogenetic implications: Geochimica et Cosmochimica Acta, v. 47, p. 925–939.

Hayashi, M., Komiya, T., Nakamura, Y., and Maruyama, S., 2000, Archean regional metamorphism of Isua supracrustal belt, southern West Greenland: Implication of a driving force of Archean plate tectonics: International Geology Review, v. 42, p. 1055–1115.

Hayes, J. M., Kaplan, I. R., and Wedeking, K. W., 1983, Precambrian organic geochemistry, preservation of the record, *in* Schopf, J. W., ed., Earth's earliest biosphere: Princeton, NJ, Princeton University Press, pp. 93–134.

Horita, J., 2001, Carbon isotope exchange in the system CO_2-CH_4 at elevated temperatures: Geochimica et Cosmochimica Acta, v. 65, p. 1907–1919.

Komiya T., Hayashi M., Maruyama S., and Yurimoto H., 2002, Intermediate-P/T type Archean metamorphism of the Isua supracrustal belt: implications for secular change of geothermal gradients at subduction zones and for Archean plate tectonics: American Journal of Science, v. 302, p. 806–826.

Komiya, T., Maruyama, S., Masuda, T., Nohda, S., Hayashi, M., and Okamoto, M., 1999, Plate tectonics at 3.8–3.7 Ga: Field evidence from the Isua accretionary complex, southern West Greenland: Journal of Geology, v. 107, p. 515–554.

Lepland, A., Arrhenius, G., and Cornell, D., 2002, Apatite in early Archean Isua supracrustal rocks, southern West Greenland: Its origin, association with graphite, and potential as a biomarker: Precambrian Research, v. 118, p. 221–241.

Ludwig, K. R, 1998, On the treatment of concordant uranium-lead ages: Geochimica et Cosmochimica Acta, v. 62, p. 665–676.

Mojzsis, S. J., Arrhenius, G., McKeegan, K. D., Harrison, T. M., Nutman, A. P., and Friend, C. R. L., 1996, Evidence for life before 3800 million years ago: Nature, v. 385, p. 55–59.

Mojzsis, S.J., Coath, C. D., Greenwood, J. P., McKeegan, K. D., and Harrison, T. M., 2003, Mass-independent isotope effects in Archean (2.5 to 3.8 Ga) sedimentary sulfides determined by ion microprobe analysis: Geochimica et Cosmochimica Acta, v. 67, p. 1635–1658.

Mojzsis, S. J., and Harrison, T. M., 2002, Origin and significance of Archean quartzose rocks at Akilia, Greenland: Science, v. 298, p. 917a.

Moorbath, S., O'Nions, R. K., and Pankhurst, R. J., 1973, Early Archean age for the Isua Iron Formation, West Greenland: Nature, v. 245, p. 138–139.

Myers J. S., 2001, Protoliths of the 3.8–3.7 Ga Isua greenstone belt, West Greenland: Precambrian Research, v. 106, p. 129–141.

Nadeau, S. L., Epstein, S., and Stolper, E., 1999, Hydrogen and carbon abundances and isotopic ratios in apatite from alkaline intrusive complexes, with a focus on carbonatites: Geochimica et Cosmochimica Acta, v. 63, p. 1837–1851.

Naraoka, H., Ohtake, M., Maruyama, S., and Ohmoto, H., 1996, Non-biogenic graphite in 3.8 Ga metamorphic rocks from the Isua district, Greenland: Chemical Geology, v. 133, p. 251–260.

Nutman, A. P., 1986, The early Archaean to Proterozoic history of the Isukasia area, southern West Greenland: Greenland Geol. Unders. Bull., v. 154, Copenhagen, 80 p.

Nutman, A. P., Bennett, V. C., Friend, C. R. L., and Rosing, M. T., 1997, ~3710 and ≥3790 Ma volcanic sequences in the Isua (Greenland) supracrustal belt; structural and Nd isotope implications: Chemical Geology, v. 141, p. 271–287.

Nutman, A. P., Friend, C. R. L., and Bennett, V. C., 2002, Evidence for 3650–3600 Ma assembly of the northern end of the Itsaq Gneiss Complex, Greenland: Implication for early Archaean tectonics: Tectonics, v. 21, p. 1–28.

Oehler, D. Z., and Smith, J. W., 1977, Isotopic composition of reduced and oxidized carbon in early Archean rocks from Isua, Greenland: Precambrian Research, v. 5, p. 221–228.

Ohmoto, H. and Kerrick, D., 1977, Devolatilization equilibria in graphitic systems: American Journal of Science, v. 277, p. 1013–1044.

Pankhurst, R. J., Moorbath, S., Rex, D. C., and Turner, G., 1973, Mineral age patterns in ca. 3700 m.y. old rocks from West Greenland: Earth and Planetary Science Letters, v. 20, p. 157–170.

Perry, E. C., Jr., and Ahmad, S. N., 1977, Carbon isotope composition of graphite and carbonate minerals from 3.8-AE metamorphosed sediments, Isukasia, Greenland: Earth and Planetary Science Letters, v. 36, p. 280–284.

Pinti D. L., Hashizume, K., and Matsuda, J., 2001, Nitrogen and argon signature in 3.8 to 2.8 Ga metasediments: Clues on the chemical state of the Archean ocean and the deep biosphere: Geochimica et Cosmochimica Acta, v. 65, p. 2301–2315.

Rollinson, H., 2003, Metamorphic history suggested by garnet-growth chronologies in the Isua Greenstone Belt, West Greenland: Precambrian Research, v. 126, p. 181–196.

Rose, N. M., Rosing, M. T., and Bridgwater, D., 1996, The origin of metacarbonate rocks in the Archean Isua supracrustal belt, West Greenland: American Journal of Science, v. 296, p. 1004–1044.

Rosing, M. T., 1999, ^{13}C-depleted carbon microparticles in >3700-Ma sea floor sedimentary rocks from West Greenland: Science, v. 283, p. 674–676.

Rosing, M. T., Rose, N. M., Bridgwater, D., and Thomsen, H. S., 1996, Earliest part of Earth's stratigraphic record: A reappraisal of the > 3.7 Ga Isua (Greenland) supracrustal sequence:. Geology, v. 24, p. 43–46.

Sano, Y., Oyama, T., Terada, K., and Hidaka, H., 1999a, Ion microprobe U-Pb dating of apatite: Chemical Geology, v. 153, p. 249–258.

Sano, Y., and Pillinger, C. T., 1990, Nitrogen isotopes and N_2/Ar ratios in cherts: An attempt to measure time evolution of atmospheric $d^{15}N$ value: Geochemical Journal, v. 24, p. 315–324.

Sano, Y., and Terada, K., 2002, Reply to Comment on "In Situ ion microprobe U-Pb dating and REE abundances of a Carboniferous conodont" by R. Romer: Geophysical Research Letters, v. 29, p. 39/1–39/2.

Sano, Y., Terada, K., and Fukuoka, T., 2002, High mass resolution ion microprobe analysis of rare earth elements in silicate glass, apatite and zircon: Lack of matrix dependency: Chemical Geology, v. 184, p. 217–230.

Sano, Y., Terada, K., Takahashi, Y., and Nutman, A. P., 1999b, Origin of life from apatite dating?: Nature, v. 400, p. 127–128.

Schidlowski, M., Appel, P. W. U., Eichmann, R., and Junge, C. E., 1979, Carbon isotope geochemistry of the 3,700-Myr-old Isua sediments, West Greenland: Implication for the Archean carbon and oxygen cycles: Geochimica et Cosmochimica Acta, v. 43, p. 189–199.

Shimizu, H., Umemoto, N., Masuda, A., and Appel, P. W. U., 1990, Sources of iron-formations in the Archean Isua and Malene supracrustals, West Greenland: Evidence from La-Ce and Sm-Nd isotopic data and REE abundances: Geochimica et Cosmochimica Acta, v. 54, p. 1147–1154.

Shimoyama, A. and Matsubaya, O., 1992, Carbon isotopic compositions of graphite and carbonate in 3.8×10^9 old Isua rocks: Chemistry Letters, v. 1992, p. 1205–1208.

Stacey, J. S. and Kramers, J. D., 1975, Approximation of terrestrial lead isotope evolution by two-stage model: Earth And Planetary Science Letters, v. 26, p. 207–221.

Takahata, N., Nishio, Y., Yoshida, N., and Sano, Y., 1998, Precise isotopic measurements of nitrogen at the sub-nano mole level: Analytical Sciences, v. 14, p. 485–491.

Tolstikhin, I. N., Kamensky, I. L., Marty, B., Nivin, V. A., Vetrin, V. R., Balaganskaya, E. G., Ikorsky, S. V., Gannibal, M. A., Weiss, D., Verhulst, A., and Demaiffe, D., 2002, Rare gas isotopes and parent trace elements in ultrabasic-alkaline-carbonatite complexes, Kola Peninsula: Identification of lower mantle plume component: Geochimica et Cosmochimica Acta, v. 66, p. 881–901.

Toyoda, K., and Tokonami, M., 1990, Diffusion of rare-earth elements in fish teeth from deep-sea sediments:. Nature, v. 345, p. 607–609.

Ueno, Y., Yurimoto, H., Yoshioka, H., Komiya, T., and Maruyama, S., 2002, Ion microprobe analysis of ca. 3.8 Ga metasediments, Isua supracrustal belt, West Greenland: Relationship between metamorphism and carbon isotopic composition: Geochimica et Cosmochimica Acta, v. 66, p. 257–1268.

Van Zuilen, M. A., Lepland, A., and Arrhenius, G., 2002, Reassessing the evidence for the earliest traces of life:. Nature, v. 418, p. 627–630.

Wedeking, K. W., Hayes, J. M., and Matzigkeit, U., 1983, Procedures of organic geochemical analysis, *in* Schopf,

J. W., ed., Earth's earliest biosphere:. Princeton, NJ, Princeton University Press, p. 93–134.
Wendt, J. I., and Collerson, K. D., 1999, Early Archean high-grade metamorphism in the Saglek-Hebron segment of the North Atlantic craton: Precambrian Research, v. 93, 281–297.
York, D., 1969, Least squares fitting of a straight line with correlated errors: Earth and Planetary Science Letters, v. 5, p. 320–324.

Appendix. Calculation of Carbon Isotopic Change of Precusor of HTC due to loss of CO_2- and CH_4-Bearing Fluid During Metamorphism

In the paper, we calculated carbon isotopic change of precursor of HTC (kerogenous material) due to loss of CO_2- and CH_4-bearing fluid, in order to discuss secondary isotope fractionation of the precursor of HTC during metamorphism. The precursor of HTC is suggested to have coexisted with H_2O, both within magnetite in quartz-magnetite BIF (43-44A) from the ISB. A Rayleigh distillation model was used for the calculation. In the model, we used following equation:

$$\delta^{13}C_{final} - \delta^{13}C_{initial} = (F^{\alpha-1} - 1) \times (\delta^{13}C_{initial} + 1000) \approx (F^{\alpha-1} - 1) \times 1000.$$

$\delta^{13}C_{final}$ and $\delta^{13}C_{initial}$ refer to the $\delta^{13}C$ values of kerogenous material after metamorphism and before metamorphism, respectively. F refers to the fraction of kerogenous material remaining, and α is the isotope fractionation factor of the C-bearing fluid relative to kerogenous material remaining. The calculation was performed under following conditions.

Metamorphic temperature

It had been long considered that the ISB underwent uniform regional metamorphism (Boak and Dymek, 1982). These authors concluded that the ISB uniformly experienced ~550°C during prograde metamorphism and later was subjected to ~460°C during retrograde metamorphism. This is because metamorphic temperature of metapelite from the ISB, calculated by garnet-biotite geothermometry, suggests equilibration at ~550°C for garnet cores, and at ~460°C for garnet rims.

However, it would be inappropriate to use the metamorphic conditions to calculate the carbon isotopic change of the kerogenous material within the BIF during metamorphism. This is because petrochemical study of garnet from each structural domain in the ISB suggests that metamorphic history of the domains that host the metapelite (Domain II, III, and IV of Rollinson, 2003) is different from that of the domain that hosts the BIF (Domain I of Rollinson, 2003).

Based on petrochemical and geothermobarometric studies of more than 1500 rock samples in Domain I, progressive metamorphic zonation was discovered in the domain (Hayashi et al., 2000; Komiya et al., 2002). The grade and temperature of each metamorphic zone in the domain is as follows: (1) Zone A (greenschist facies); (2) Zone B (albite-epidote-amphibolite facies; 400–420°C; Hayashi et al., 2000); (3) Zone C (lower amphibolite facies: up to 480°C; Appel et al., 2001); (4) Zone D (upper amphibolite facies: up to 550°C; Hayashi et al., 2000).

The metamorphic temperature of each zone was estimated from garnet-biotite geothermometry (Hayashi et al., 2000, Appel et al., 2001). Because most garnets from Domain I show normal zoning and do not contain evidence of retrogression (Hayashi et al., 2000; Rollinson, 2003), the estimated temperature of each zone probably reflects the temperature at peak metamorphic conditions. Because the BIF is from Zone A, the metamorphic temperature of the BIF is suggested to be ~400°C. Thus, we calculated the carbon isotopic change of the kerogenous material within the BIF at 400°C.

Total fluid pressure

We assumed that the total fluid pressure equals the metamorphic pressure. A pressure of ~5 kbar for Domain I was estimated from garnet-hornblende-plagioclase-quartz geobarometry (Hayashi et al., 2000). Thus, we used 5 kbar for our calculation.

Oxygen fugacity and α value

We assumed that oxygen fugacity of the kerogenous material-H_2O system within magnetite is higher than that determined by the FMQ buffer, and lower than that determined by the graphite buffer (Fig. 7A). Within the range of oxygen fugacity of the kerogenous material–H_2O system, the CO_2/CH_4

molar ratio of fluid released from the kerogenous material was estimated (Ohmoto and Kerrick, 1977). To calculate the α value, we used $\alpha_{CO2\text{-}graphite}$ and $\alpha_{CH4\text{-}graphite}$ values from Chacko et al. (1991) and Horita (2001), respectively.